WILEY

# Multi-decadal morpho-sedimentary dynamics of the largest Changjiang estuarine marginal shoal: Causes and implications

Wen Wei[1] | Zhijun Dai[1,2] (iD) | Xuefei Mei[1] | Shu Gao[1] | J. Paul Liu[3]

[1] State Key Laboratory of Estuarine and Coastal Research, East China Normal University, Shanghai 200062, PR China

[2] Laboratory for Marine Geology, Qingdao National Laboratory for Marine Science and Technology, Qingdao 266100, PR China

[3] Department of Marine, Earth, and Atmospheric Sciences, North Carolina State University, Raleigh, NC 27695, USA

**Correspondence**
Z. Dai, State Key Lab of Estuarine and Coastal Research, East China Normal University, Shanghai 200062, China.
Email: zjdai@sklec.ecnu.edu.cn

## Abstract

Understanding the long-term evolution of estuarine shoals given natural variations and human modifications is a key issue for wetland protection and shoal management. Here, the multi-decadal (1958–2013) morpho-sedimentary dynamics of the Nanhui Shoal (NHS), the largest Changjiang estuarine marginal shoal, are studied using a suite of hydrological, sedimentological, and bathymetric data. The results show that the tidal flow regime and sedimentary mode around the NHS changed slightly after the 1980s. Moreover, the NHS experienced a siltation-induced volume increase of $4.1 \times 10^8$ m$^3$, concentrated in the landward region, and seaward progradation, producing an increase in gross area of 33 km$^2$, during 1958–2013. Even so, the actual tidal flat resource decreased by 29% due to the reclamation of 202 km$^2$. Transition in the development of the NHS is detected: a planar geometry transformation from a triangular cusp to an arcuate cusp during 1958–1989; vertical siltation in the landward region under a stable arcuate-shaped geometry thereafter. Furthermore, a steeply sloping profile with grades of 2–11‰ formed in the northern section, which limits future reclamation to 80 km$^2$ there. Estuarine regime adjustment, inducing hydrodynamic alterations in the South Passage, dominated the geometric changes in the NHS during 1958–1989, whereas substantial siltation promotion projects led to the landward siltation after 1989. The decrease in sediment input downstream of the Three Gorges Dam has played a minor role in the shoal evolution. This work provides new insights into the long-term morpho-sedimentary responses of estuarine shoals to natural and artificial forcings and their implications for shoal exploitation.

### KEYWORDS

artificial interference, Changjiang Estuary, estuarine shoal, morpho-sedimentary dynamics, natural variations

## 1 | INTRODUCTION

Estuarine shoals, which develop at the interfaces between fluvial systems and open-coast regimes, perform vital ecological functions, including pollution removal, habitat provision, and hazard mitigation (Kirwan & Megonigal, 2013). Additionally, estuarine shoals are key areas of land for urban expansion (Hoeksema, Vlotman, & Madramootoo, 2007; Wei et al., 2017). In recent decades, estuarine

shoals have suffered from dramatic changes in both natural and artificial forcings (Giosan, Syvitski, Constantinescu, & Day, 2014; Syvitski et al., 2009). Understanding the long-term morpho-sedimentary development of estuarine shoals in the face of natural variations and artificial interference is therefore a key issue for estuarine wetland protection and shoal resource management.

Many studies indicate that the morpho-sedimentary dynamics of estuarine shoals result from complex interactions among sediment

inputs, local hydrodynamics (wave and fluvial and tidal flow), and certain biochemical factors and can exhibit fluctuations on tidal, seasonal, and multi-year cycles (Verney, Lafite, & Bruncottan, 2009; Wei et al., 2017; Wei, Mei, Dai, & Tang, 2016; Wright & Coleman, 1974). Natural variations, such as the estuarine regime adjustment resulting from channel shifts, avulsions, or bifurcation alterations, may have far-reaching effects on the long-term evolution of estuarine shoals. Examples of evolving estuaries include the Mississippi (Törnqvist et al., 1996) and Huanghe (Syvitski & Saito, 2007) estuaries, in which the depocenters of the deltas have migrated with successive shifts in the courses of the rivers and in which shoals outside active main channels tend to experience more intense accretion. In the Changjiang Estuary, changes in the water/sediment partitioning between channels in response to estuarine regime adjustment have been found to play a significant role in shoal growth (Dai, Liu, Wei, & Chen, 2014; Yun, 2010).

Considering the occurrence intervals of avulsions, which may be long in modern rivers (Stouthamer & Berendsen, 2001), estuarine shoals have become more likely to be impacted by intensive anthropogenic activities in recent decades (e.g., Anthony et al., 2015; Syvitski et al., 2009). For example, upstream damming has resulted in a sharp decrease in the riverine sediment discharge and thus the recession of estuarine shoals in the Nile (Fanos, 1995), Niger (Abam, 1999), Arno (Pranzini, 2001), Rhône (Sabatier et al., 2006), Huanghe (Syvitski & Saito, 2007), Mississippi (Blum & Roberts, 2009), Po (Simeoni & Corbau, 2009), Changjiang (Yang, Milliman, Li, & Xu, 2011), Danube (Tatui, Vespremeanu-Stroe, & Preoteasa, 2014), Mekong (Anthony et al., 2015), Guadalfeo (Bergillos, Rodríguez-Delgado, Millares, Ortega-Sánchez, & Losada, 2016), and Volta (Anthony, Almar, & Aagaard, 2016) deltas. In addition, the extensive construction of artificial structures within estuaries, including embankments, dikes, bridges, and groynes, tends to reduce tidal prisms, weaken regional tidal flow, and facilitate shoal accretion, as manifested in the Mersey Estuary, northern England (van der Wal, Pye, & Neal, 2002), the Changjiang Estuary, China (Wei et al., 2016), and the Seine Estuary, France (Cuvilliez, Deloffre, Lafite, & Bessineton, 2009). Reclamation projects generally lead to the degradation of supratidal and intertidal flats; examples include the Isahaya Reclamation Project in Japan (Hodoki & Murakami, 2006), the Saemangeum Reclamation Project in South Korea (Son & Wang, 2009), and large-scale reclamation projects along the coast of The Netherlands (Hoeksema et al., 2007). Moreover, reclamation around bifurcation can induce flow diversion changes, which is a major cause of shoal accretion in the North Branch of the Changjiang Estuary (Dai, Fagherazzi, Mei, Chen, & Meng, 2016). The multi-decadal morpho-sedimentary response of estuarine shoals to artificial interference has gained increasing attention worldwide, especially the detection of morphological changes and the assessment of the causal mechanisms through field investigations (e.g., Anthony et al., 2015, 2016; Bergillos et al., 2016; Fanos, 1995; Sabatier et al., 2006; Simeoni & Corbau, 2009; van der Wal et al., 2002; van der Wal & Pye, 2003; Yang et al., 2011) and numerical models (e.g., Canestrelli, Lanzoni, & Fagherazzi, 2014; Dam, van der Wegen, & Labeur, 2016; Pittaluga et al., 2015; Rossington, Nicholls, Stive, &

Wang, 2011; Todeschini, Toffolon, & Tubino, 2008). Research regarding the integrated impacts of engineering works in catchments and within estuaries on estuarine shoal evolution has also been conducted (e.g., Cuvilliez et al., 2009; Kim, Choi, & Lee, 2006; van der Wal et al., 2002; Wei et al., 2016; Wei et al., 2017). However, little information is available on the long-term development and transformations of the morpho-sedimentary dynamics of estuarine shoals under coupled natural and artificial forcings, especially in the Changjiang Estuary.

In this study, the Nanhui Shoal (NHS), the largest marginal shoal of the Changjiang Estuary, is selected to examine the detailed morpho-sedimentary processes of estuarine shoals on a multi-decadal scale, especially the coupled hydrological, sedimentological, and geomorphological responses to natural variations and human modifications and possible developmental transitions. Based on the bathymetric data covering the period 1958–2013 and the associated hydrological and sedimentological data, our study aims to (a) detect the multi-decadal changes in hydrology, sedimentation, and geomorphology of the NHS; (b) identify the factors that impact the development of the NHS; and (c) analyze the implications of the evolution of the NHS. This work addresses the development of an estuarine shoal in response to dramatic changes in natural and artificial forcings and provides important information on long-term morpho-sedimentary dynamics for use in shoal management.

## 2 | MATERIALS AND METHODS

### 2.1 | Study area

The NHS, located on the southern flank of the Changjiang Estuary, plays a vital role in storm mitigation and land production for Shanghai (Figure 1). The NHS has exhibited seaward progradation of more than 60 km over the past thousands of years (Yun, 2010); however, it has suffered from significant alterations in both natural and artificial forcings over recent decades. For example, an extreme flood in 1954 resulted in the avulsion of the North Passage and may have induced a long-term adjustment of the estuarine regime (Yun, 2010). The construction of the Three Gorges Dam (TGD) resulted in a 70% decrease in the riverine sediment discharge after 2003 (Dai et al., 2014). The implementation of the Deep Waterway Project (DWP; 1998–2010) significantly altered the material diversions between the North and South passages (Hu & Ding, 2009). Furthermore, reclamation is widely conducted, especially on the NHS (Wei et al., 2015). Thus, the NHS is a key area for exploring the long-term morpho-sedimentary adjustments of estuarine shoals in response to natural variations and human modifications.

The width of the NHS increases downstream from the upstream edge to the shoal cusp, beyond which the shoal width decreases dramatically (Figure 2a). Fluvial controls on the NHS are mostly confined to the region upstream of the Dazhi River. The NHS experiences a meso-tide, with a mean tidal range of 3.2 m and a spring tidal range of 4 m (at Luchaogang). The wave activity is relatively
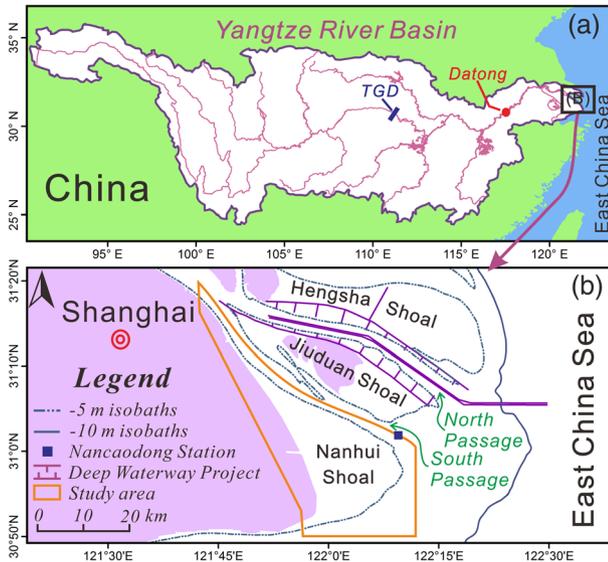
**FIGURE 1** (a) The Changjiang River Basin, including the locations of the Three Gorges Dam and the Datong gauge station, and (b) the southern Changjiang Estuary, including the main shoals (the Hengsha Shoal, Jiuduan Shoal, and Nanhui Shoal), channels (the North Passage and South Passage), the Deep Waterway Project, and the study area [Colour figure can be viewed at wileyonlinelibrary.com]

## 2.2 | Hydrological data

Data on annual water and sediment discharge at the Datong gauge station (the tidal limit of the Changjiang Estuary; Figure 1a) over the period 1953–2013 were collected from the Bulletin of China River Sediment (www.cjh.com.cn/). These data portray the response of the Changjiang riverine loads to human activities in the catchment. Data on the monthly suspended sediment concentration (SSC) at the Nancaodong gauge station (Figure S1) between 2006 and 2009 were obtained from the Estuarine and Coastal Science Research Center of Shanghai (http://www.ecsrc.org/). These data provide information on the quantities of suspended sediment associated with the accretion of the NHS. Data on the ebb flow diversion ratio of the South Passage between 1964 and 2013 were acquired from the Changjiang Estuary Waterway Administration Bureau (http://www.cjkhd.com/) and are used to detect changes in hydrodynamics of the South Passage.

The wave dynamics around the NHS were modelled using the TELEMAC2D-TOMAWAC modelling system, first established by Zhang, Townend, Zhou, and Cai (2016). The typical summer and winter scenarios were considered based on wind data from the Quick Scatterometer (http://www.remss.com/missions) and daily water discharge data (at Datong gauge station) from the Changjiang Water Resources Commission of the Ministry of Water Resources between 2002 and 2012. Finally, data on the tidal flow and SSC around the NHS monitored during spring tides in 9/1994, 9/2003, and 8/2006 were acquired (Table 1, Figure S1) to document tidal dynamics and suspended sediment transport on the NHS. The current velocity and SSC at 0%, 20%, 40%, 60%, 80%, and 100% of the actual water depth were measured hourly in the surveys, using an acoustic Doppler current profiler (Teledyne RD Instruments) and OBS-3A (Campbell Scientific), respectively. A surficial tidal current rose diagram was produced for the different years, and the bed
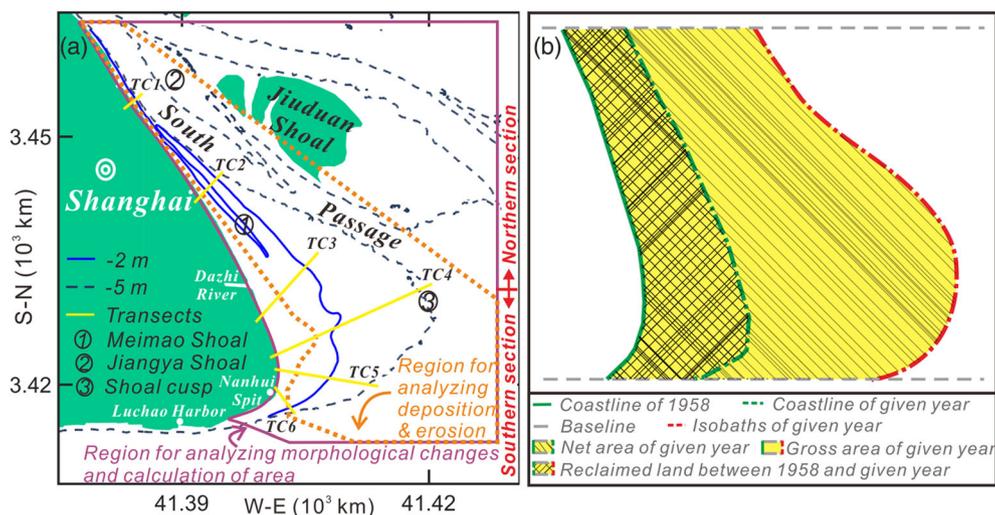
intense here, showing a mean wave height of 1 m and a recorded highest wave height of 6 m during storms (off the Nanhui Spit). From the Nanhui Spit upstream, the shoal is less exposed and thus experiences weaker wave action. Extreme floods have occasionally occurred in the estuary, and these events have played a significant role in estuarine geomorphology (Yun, 2010). Surface sediments on the shoal are sandy to silty and are the coarsest among the major shoals in the Changjiang Estuary.



**FIGURE 2** (a) Map showing the Jiangya Shoal, the Meimao Shoal, the locations of the transects, and the regions for analysis of morphological changes, deposition/erosion, and area variations and (b) a sketch diagram depicting the calculation of the net and gross areas [Colour figure can be viewed at wileyonlinelibrary.com]

**TABLE 1** Tidal current and suspended sediment concentration data for the Nanhui Shoal

| Date | Tidal regime | Site number |
|------|-------------|-------------|
| 9/1994 | Spring tide | 9 |
| 9/2003 | Spring tide | 21 |
| 8/2006 | Spring tide | 14 |

shear stress was calculated following Daniel (1985) and Qiao, Zhang, and Xu (2010). In addition, the net suspended sediment transport vector was computed following Zhang (1988). Due to variations in the Changjiang water discharge, wind conditions, and locations of the hydrological sites, only a qualitative assessment of the spatial distribution of the current vector, maximum bed shear stress, and suspended sediment transport direction during the spring tidal cycles is conducted.

## 2.3 | Sedimentological data

Data on the grain size of the surface sediments within the NHS in 1982, 2004, and 2011 (Table 2; Figure S2) were collected to define changes in the grain size distribution. All of the sediment samples were collected at depths ranging from 1 to 5 cm and analyzed for grain size in the laboratory. The samples collected in 1982 were analyzed using a sieving and settlement method, and the others were analyzed using a Mastersizer 2000 grain size analyzer (Malvern Instruments Ltd.). Therefore, the median grain size ($D_{50}$) data of the sediments (Folk & Ward, 1957) collected in 1982 are used only to determine the spatial distribution of the surface sediments, and the others are used to quantitatively assess sediment grain size variations over time.

## 2.4 | Bathymetric data

Bathymetric data covering the period 1958–2013 were collected (Table 3; Figure S3), and these data serve as the core data for exploring the multi-decadal development of the NHS and its resource abundance (e.g., Blott, Pye, van der Wal, & Neal, 2006; van der Wal & Pye, 2003). All of the bathymetric data were first transferred into the Beijing 1954 coordinates and calibrated to the Wusong Datum (which refers to the lowest water level) on the ArcGIS 10.2 platform following Blott et al. (2006). A digital elevation model with a cell size of 50 m and isobaths of 0, −2, and −5 m was generated on the MATLAB 2012 platform using the triangulated

**TABLE 2** Sediment grain size data for the Nanhui Shoal

| Date | Sample number | Grain size analysis method |
|------|--------------|---------------------------|
| 6/1982; 12/1982 | 68 | Sieving and settlement method |
| 7/2004 | 48 | Laser particle analysis |
| 6/2011 | 39 | Laser particle analysis |

**TABLE 3** Bathymetric data for the Nanhui Shoal

| Year[a] | Data source | Scale | Survey period |
|---------|-------------|-------|---------------|
| 1958 | Navigational chart published by NGDCNH[b] | 1:100,000 | 1958 |
| 1978 | Navigational chart published by NGDCNH | 1:120,000 | 1976–1978 |
| 1984 | Navigational chart published by NGDCNH | 1:120,000 | 1983–1984 |
| 1989 | Navigational chart published by NGDCNH | 1:120,000 | 1987–1989 |
| 1997 | Navigational chart published by HBCE[c] | 1:50,000 | 1997 |
| 2002 | Bathymetric survey conducted by CEWAB[d] | 1:120,000 | 2002 |
| 2009 | Navigational chart published by SIGS[e] | 1:50,000 | 2009 |
| 2013 | Bathymetric survey conducted by CEWAB | 1:10,000 | 2013 |

[a]Year represented by the corresponding bathymetric data in this study.
[b]Navigation Guarantee Department of the Chinese Navy Headquarters (http://www.ngd.gov.cn/).
[c]Hydrological Bureau of the Changjiang Estuary, China (http://www.cjh.com.cn/).
[d]Changjiang Estuary Waterway Administration Bureau, Ministry of Transportation (http://www.cjkhd.com/).
[e]Shanghai Institute of Geological Survey, China (http://www.silrs.com/).

irregular network interpolation method (Figure 2a). The changes in the net area and the gross area were then analyzed. The net area was calculated as the area of the envelope defined by the coastline (as well as the newest seawall digitized from the charts) and the isobaths corresponding to a given year, which yields a quantitative assessment of the actual tidal flat resource (Wei et al., 2015; Yun, 2010). The gross area was computed as the area of the envelope defined by a fixed coastline (that of 1958) and the isobaths corresponding to a given year to quantify the progradation/retreat of the NHS. The gross area, therefore, is equal to the sum of the net area and the area of land reclaimed since 1958. Notably, the area of the reclaimed land is usually different from that of the conducted reclamation projects (reclaimed shoals) because reclamation projects in the Changjiang Estuary are conducted to depths of −2 m. Assessments of deposition/erosion and volume variations were conducted within a region common to the data from different years (Figure 2 a). Six transects, the first three across the northern section and the last three across the southern section (Figure 2a), were extracted to detect profile changes.

A statistical analysis was conducted to determine the accuracy of the related morpho-sedimentary dynamic analyses. The average measurement error of modern fathometers is approximately 2 to 5 cm for water depths less than 5 m and 1% for depths exceeding 5 m (Chen & Yang, 2010; Dai et al., 2014). Considering the largest measurement errors, the calculated shoal area above −2 and −5 m

and the volume of the NHS exhibit errors within 3%, 1%, and 2%, respectively. For the region above 0 m, a measurement error of 5 cm might be impractical considering the relatively shallow water depth; thus, a measurement error of 2 cm is introduced, producing a calculation error of 5% to 8%. Although positioning error also exists and is 50 m in the data of 1958, 1978, 1984, and 1989 and 1 m for the recently collected data (Dai et al., 2014), the high density (5–20 points per km$^2$) of the elevation points in the bathymetric investigations limits the calculation error.

# 3 | RESULTS

## 3.1 | Changes in the hydrological and sedimentological environment of the NHS

### 3.1.1 | Wave and tidal dynamics

The distributions of the maximum significant wave heights in summer and winter are similar (Figure 3). Large wave heights (greater than 0.5 m) occur in the region between the Dazhi River and the Nanhui Spit, and wave dissipation, manifested by a high wave height

gradient, occurs north of the Dazhi River and south of the Nanhui Spit. The tidal flow has always been characterized by a bidirectional current along the South Passage north of the Dazhi River, a transmeridional bidirectional flow south of the Nanhui Spit, and a rotating flow in between (Figure 4a). The maximum bed shear stress induced by tidal flow is larger in areas of deep water than in the shoal region and is minimal within the −2- to −5-m isobaths between the Dazhi River and the Nanhui Spit (Figure 4b). The net suspended sediment transport shows a downstream trend in the region deeper than −2 m but an upstream trend in the shallower region north of the Dazhi River and an eastward trend just outside the Dazhi River (Figure 4c). South of the Dazhi River, suspended sediment is transported northeastward in the region deeper than −5 m and landward in the shallower region.

### 3.1.2 | Sediment grain size

The median grain size of the surface sediments within the NHS exhibits a similar distribution mode over the period 1982–2011, with scattered low values centered outside the Dazhi River and around the Nanhui Spit (Figure 5). However, differences exist in the median grain size distribution: the low-value center outside the Dazhi River became more
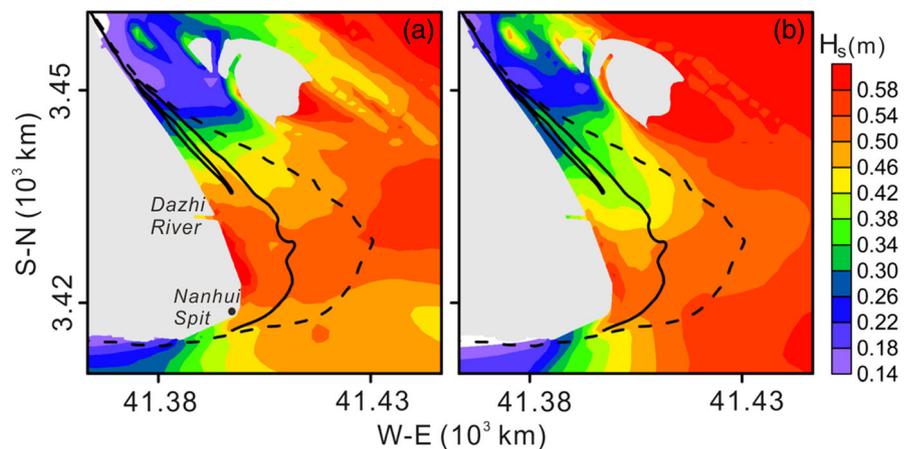


FIGURE 3 The spatial distribution of the maximum significant wave heights around the Nanhui Shoal during a tidal cycle in (a) summer and (b) winter [Colour figure can be viewed at wileyonlinelibrary.com]
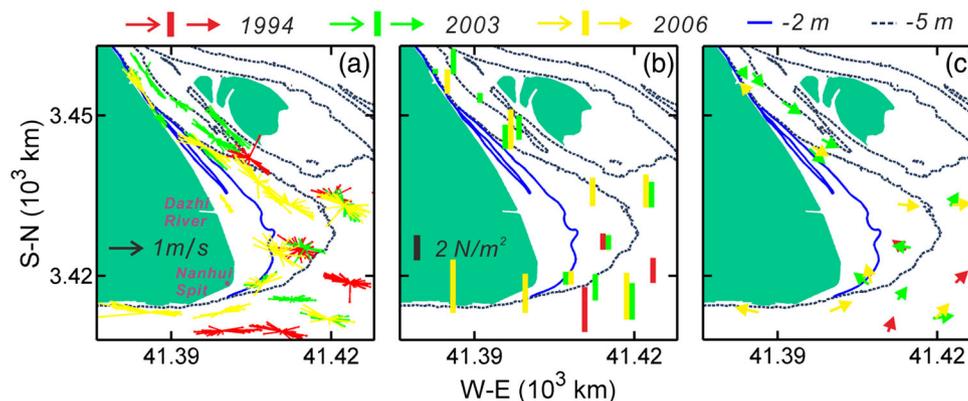


FIGURE 4 The spatial distribution of tidal flow characteristics around the Nanhui Shoal: (a) tidal flow rose diagram, (b) maximum bed shear stress, and (c) net suspended sediment transport rate [Colour figure can be viewed at wileyonlinelibrary.com]
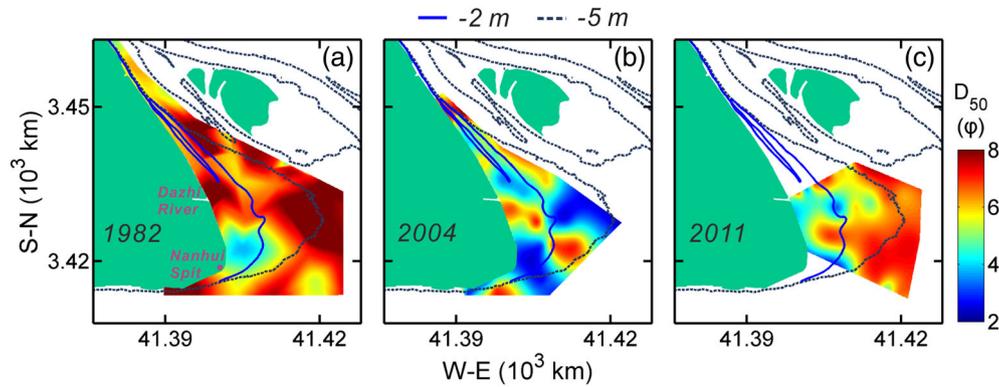
**FIGURE 5** The spatial distribution of the median grain size of the surface sediments within the Nanhui Shoal in (a) 1982, (b) 2004, and (c) 2011 [Colour figure can be viewed at wileyonlinelibrary.com]

prominent in 2004 and expanded southeastward in 2011. The low-value center around the Nanhui Spit expanded southeastward after 2004. The high-value region around the shoal cusp transformed to a low-value center in 2004 and became a high-value region again in 2011. In addition, the area of the high-value region in 2011 was larger than that in 2004, indicating a gradual fining of the surface sediments.
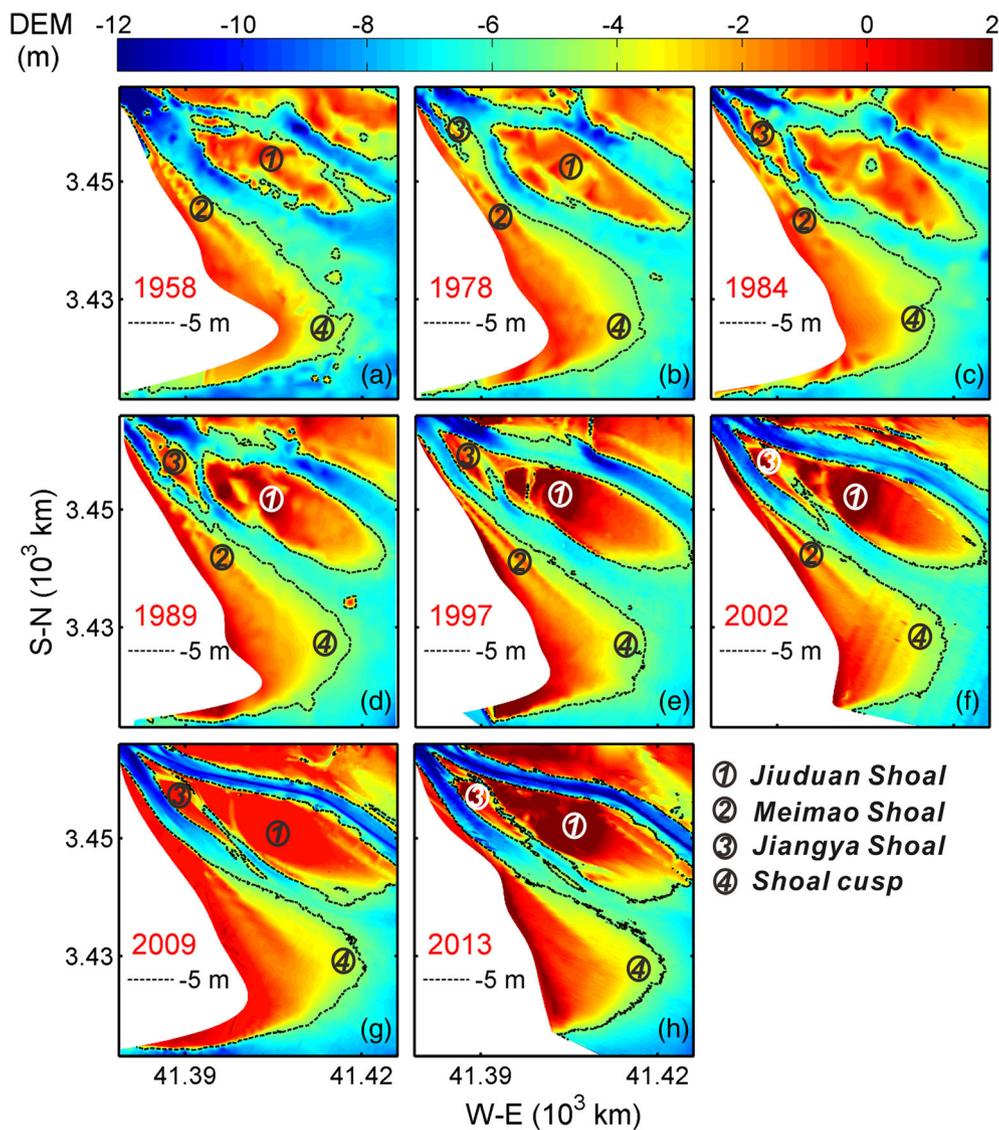


**FIGURE 6** A representative digital elevation model (DEM) depicting the morphological changes in the Nanhui Shoal over the period 1958–2013 [Colour figure can be viewed at wileyonlinelibrary.com]
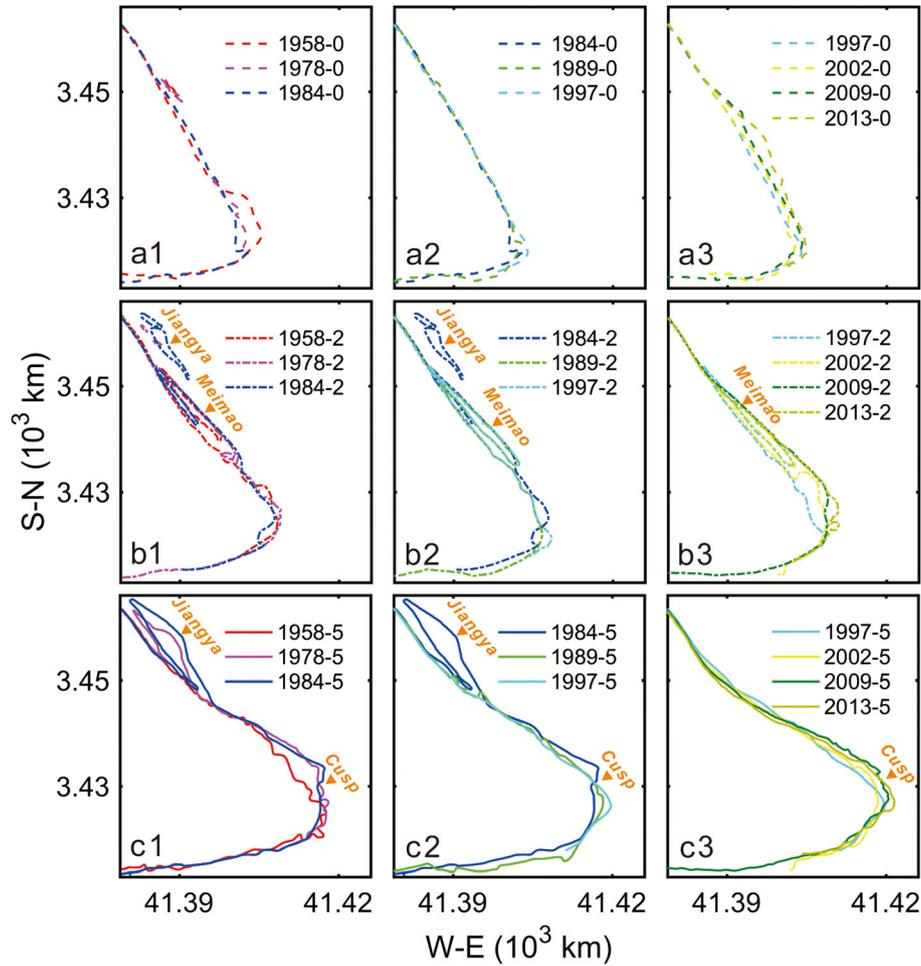
**FIGURE 7** (a1–a3) Changes in the 0-m isobaths of the Nanhui Shoal over the periods 1958–1984, 1984–1997, and 1997–2013; (b1–b3) and (c1–c3) show the changes in the −2- and −5-m isobaths, respectively [Colour figure can be viewed at wileyonlinelibrary.com]

## 3.2 | Changes in morphology and sedimentation of the NHS

### 3.2.1 | Morphological changes

Over the period 1958–1989, the NHS experienced dramatic changes in its planar geometry. Specifically, the NHS expanded seaward dramatically from 1958 to 1978 as the South Passage narrowed, with the triangular cusp transforming to an arcuate shape, which became slightly bulged in 1984 and rotated southward between 1984 and 1989 (Figures 6a–d and 7c1–c2). Furthermore, a 36-km$^2$ mound (the embryonic Jiangya Shoal) formed in the northern section in 1978, resulting in a curved South Passage, grew to 57 km$^2$ in 1984 and separated from the NHS in 1989, making the South Passage straight again but bifurcated (Figure 6c). The −2-m isobaths in the northern section also expanded and contracted from 1978 to 1989 and were highly dynamic in response to the evolution of the tidal ridge, namely, the Meimao Shoal (Figures 6a–d and 7c1–2). In the southern section, the −2-m isobaths exhibited a slight retreat, whereas the 0-m isobaths retreated significantly in the region between the Dazhi River and the Nanhui Spit (Figure 7a1–2). From 1989 to 2013, although the formerly planar geometry changed

slightly and despite a more bulged cusp and a narrower flat in the northern section, the NHS experienced significant siltation in the landward region (Figures 6d–h and 7c2–3). The Jiangya Shoal migrated downstream continuously and merged with the Jiuduan Shoal in 1997. The shoal cusp migrated alternately northward and southward over the periods 1997–2002 and 2009–2013. The −2-m isobaths in the southern section advanced seaward significantly between 1997 and 2002, whereas those in the northern section remained stable. The trough west of the Meimao Shoal became infilled in 2009, causing the −2-m isobaths of the Meimao Shoal and the upper NHS to merge (Figure 7b3). The 0-m isobaths advanced dramatically after 1997, except in the northern section (Figure 7a3).

### 3.2.2 | Deposition and erosion

From 1958 to 1978, the NHS experienced siltation outside the −2-m isobaths, especially around the Jiangya Shoal (Figure 8a). Accordingly, the volume of the NHS increased by 1.4 × 10$^8$ m$^3$ (Figure 8a,h). Despite erosion of 1 m inside the shoal cusp, continuous siltation exceeding 2 m around the Jiangya Shoal resulted in a volume increase of 0.3 × 10$^8$ m$^3$ from 1978 to 1984 (Figure 8b,h). The subsequent
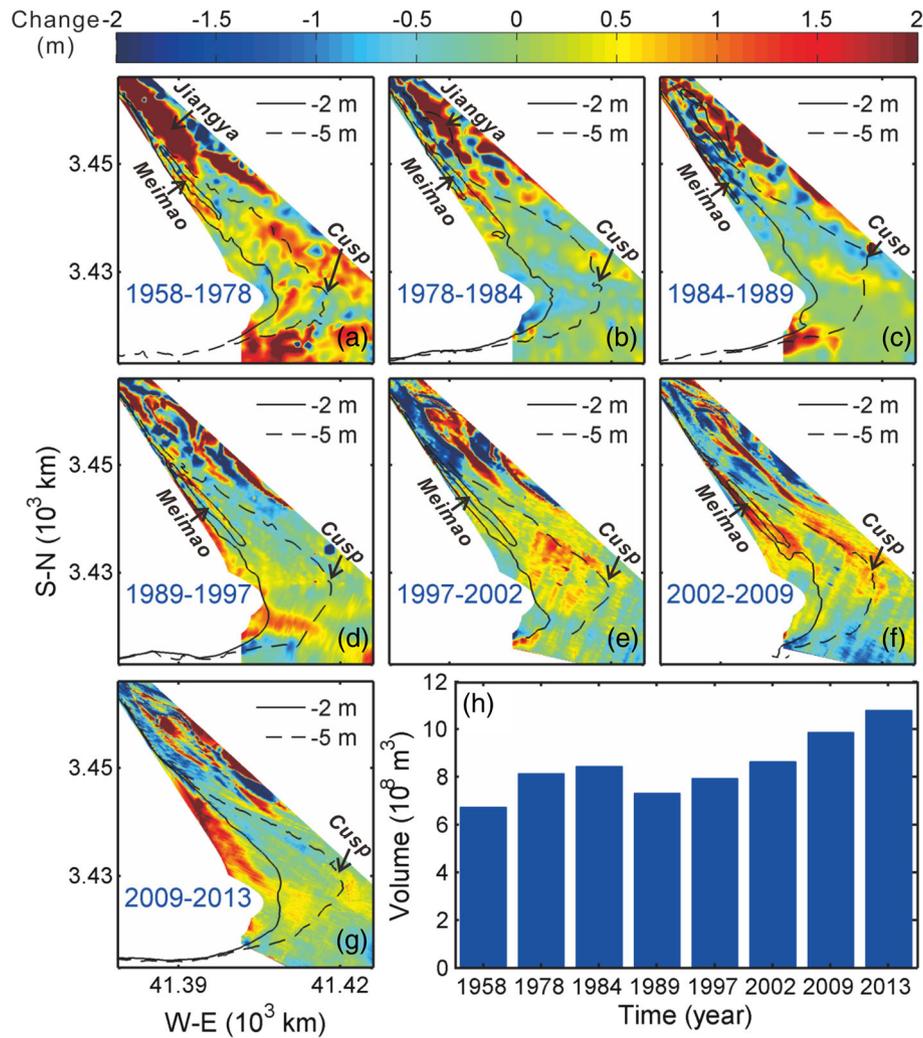
**FIGURE 8** Changes in the (a–g) siltation and (h) volume of the Nanhui Shoal between 1958 and 2013 [Colour figure can be viewed at wileyonlinelibrary.com]

erosion along with the separation of the Jiangya Shoal, however, decreased the NHS's volume from $8.4 \times 10^8$ m$^3$ in 1984 to $7.3 \times 10^8$ m$^3$ in 1989 (Figure 8c,h). From 1989 to 2013, significant siltation occurred over the entire shoal, except in the region deeper than −2 m in the northern section; thus, the volume increased to $10.8 \times 10^8$ m$^3$ in 2013 (Figure 8). Over the course of this process, although the locations of the siltation centers varied over time, erosion in the northern section was always accompanied by deposition in the southern section, especially between 1997 and 2013 (Figure 8). In addition, the southern edge of the NHS experienced alternating erosion and deposition over the period 1958–2013 (Figure 8a–g).

### 3.2.3 | Profile changes

Over the period of 1958–2013, the three transects across the northern section of the NHS display siltation in the landward region but erosion or minor changes in the seaward region, with the formation of a steep slope (Figure 9). For example, TC1 showed a gentle slope of 4.9‰ in 1958, a mound above −2 m between 1978 and 1984

related to the development of the Jiangya Shoal, and finally, a steep slope of 11.1‰ in 2013 due to siltation in the region shallower than −2 m and erosion in areas deeper than −2 m (Figure 9a). Similarly, TC2 presented a gentle slope of 0.6‰ above 1 m, followed by a steep slope between 1 and −5 m in 2013 (Figure 9b). Significant siltation in the region shallower than −3.5 m along TC3 resulted in the development of a steep slope of 2.2‰ between −1 and −3.5 m (Figure 9c). The gradient of the steep slope decreased downstream in the northern section, whereas the width of the flat landward of it increased. The transects in the southern section generally experienced widespread siltation and tended to develop into gently sloping profiles. Siltation on both sides of TC4 led to a progradation of ~4 km and a gentle slope in 2013 (Figure 9d). TC5 and TC6 both transformed from an 'S' shape to a gently sloping profile with overall siltation reaching 2 m.

### 3.2.4 | Area variations

The gross area, which represents the progradation/retreat of the NHS, displays an overall increasing trend over the period
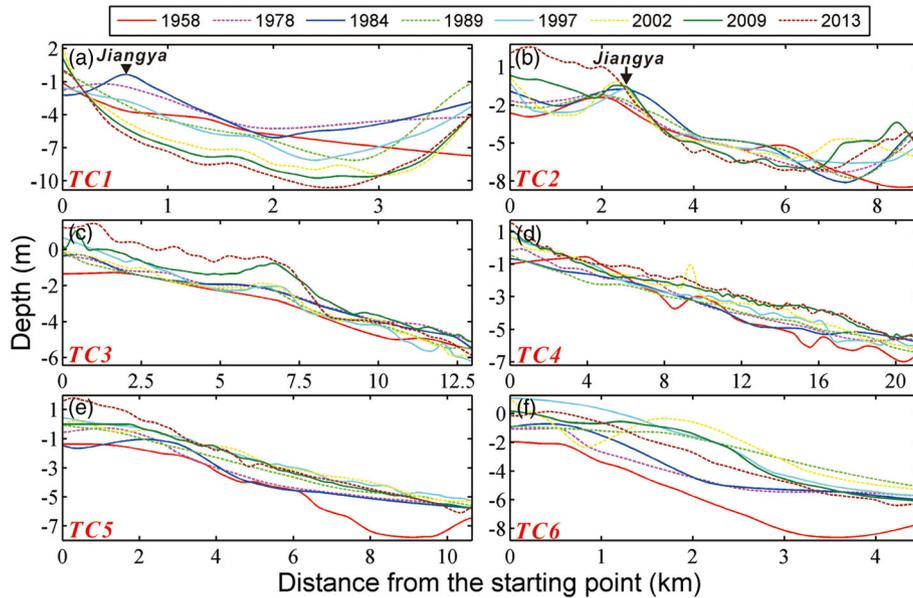
**FIGURE 9** Changes in transects over the Nanhui Shoal. See Figure 2a for locations [Colour figure can be viewed at wileyonlinelibrary.com]

1958–2013, with the areas above 0, −2, and −5 m increasing by 69 km² (33%), 83 km² (26%), and 33 km² (6%), respectively (Figure 10). Stage changes are detected in the time series of the gross area: the gross area above 0 m decreased by 28 km² from 1958 to 1984 but increased by 107 km² from 1984 to 2013, whereas that above −2 m increased by 38 km² from 1958 to 1984, decreased by 43 km² over 1984–1989, and increased continuously after 1989. The gross area above −5 m increased by 107 km² from 1958 to 1984, decreased by 71 km² from 1984 to 1989, and

changed little over 1989–2013. However, the net area, representing the actual tidal flat resources, decreased dramatically from 1958 to 2013 (Figure 10). Specifically, the net area above 0 m decreased from 211 to 78 km² over 1958–2013 (i.e., by 63%), that above −2 m decreased from 325 to 206 km² (37%), and that above −5 m decreased from 586 to 417 km² (29%). The decrease in the net area above 0 m occurred mainly over 1997–2009, that above −2 m occurred mainly over 1978–1989 and 2002–2009, and that above −5 m occurred mainly over 1984–1997 and 2002–2013.
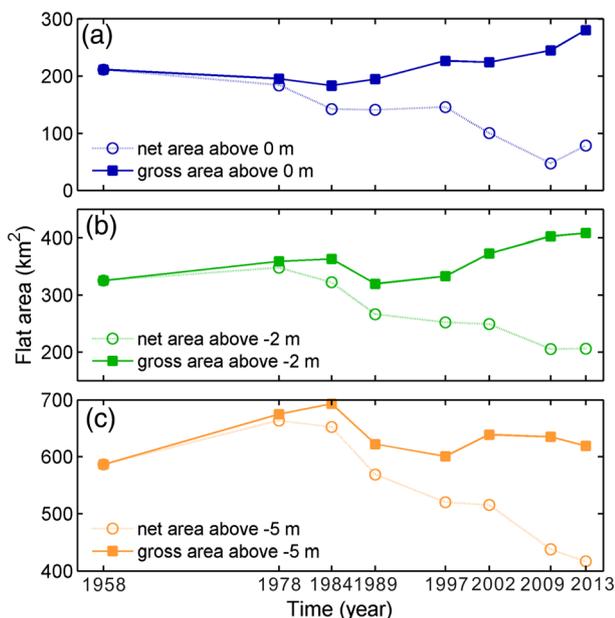
## 3.3 | Natural variations and human modifications associated with the NHS

### 3.3.1 | Riverine loads

Over the past 55 years, the sediment discharge from Changjiang has decreased from greater than 470 mt year⁻¹ during 1953–1984 to below 150 mt year⁻¹ after 2003, representing a decrease of 70%, because of the operation of the TGD (Figure 11a). Even so, the SSC at Nancaodong remained stable during 2006–2009 (Figure 11b). A significant annual cycle is detected for the SSC, with monthly mean values of 0.69–0.89 and 0.42–0.53 kg m⁻³ in the flood and drought seasons, respectively (Figure 11b). The Changjiang water discharge experiences minor fluctuations despite the extreme flood of 1954 and 1998, with no significant decreasing trends even after the construction of the TGD.

### 3.3.2 | Flow diversion

The ebb flow diversion ratio of the South Passage was highly variable from 1958 to 2013 (Figure 12) and changed in relation to the alterations in the estuarine regime. From 1958 to 1978, the ratio
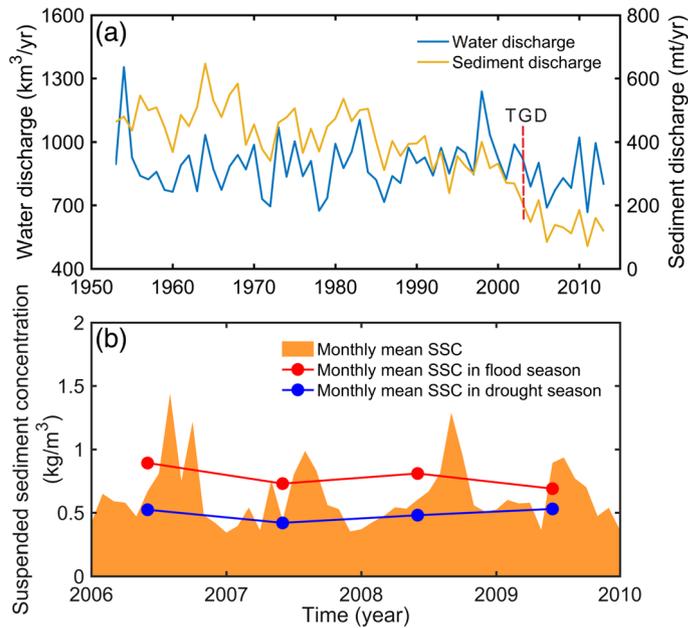


**FIGURE 10** Changes in the net and gross areas of the Nanhui Shoal over the period 1958–2013, with (a) above 0 m, (b) above −2 m, and (c) above −5 m [Colour figure can be viewed at wileyonlinelibrary.com]

**FIGURE 11** (a) Changes in the annual water and sediment discharge of the Changjiang River measured at Datong and (b) variations in the monthly suspended sediment concentration (SSC) monitored at Nancaodong. TGD, Three Gorges Dam [Colour figure can be viewed at wileyonlinelibrary.com]
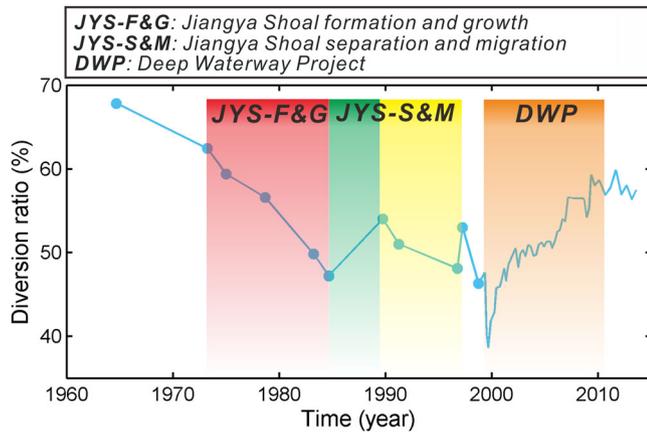


**FIGURE 12** Variations in the ebb flow diversion ratio of the South Passage over the period 1964–2013 [Colour figure can be viewed at wileyonlinelibrary.com]

decreased by 11% along with narrowing and bending of the South Passage. Thereafter, the ratio exhibited a continuous decrease from the late 1970s to the early 1980s and an increase of 7% between 1984 and 1989 in response to continuous channel bending and subsequent channel straightening induced by the formation and separation of the Jiangya Shoal, respectively. The ratio then showed large fluctuations until 1997, when the Jiangya Shoal migrated downstream. In addition, the ratio increased by 18.9% over 1999–2013 in response to the implementation of the DWP.

### 3.3.3 | Reclamation projects

Large-scale reclamation projects were conducted within the NHS during the period 1958–2013 (Figure 13a). Specifically, 53 km² of land was reclaimed from 1958 to 1989, and the reclamation area increased significantly to 149 km² from 1989 to 2013. Notably, siltation
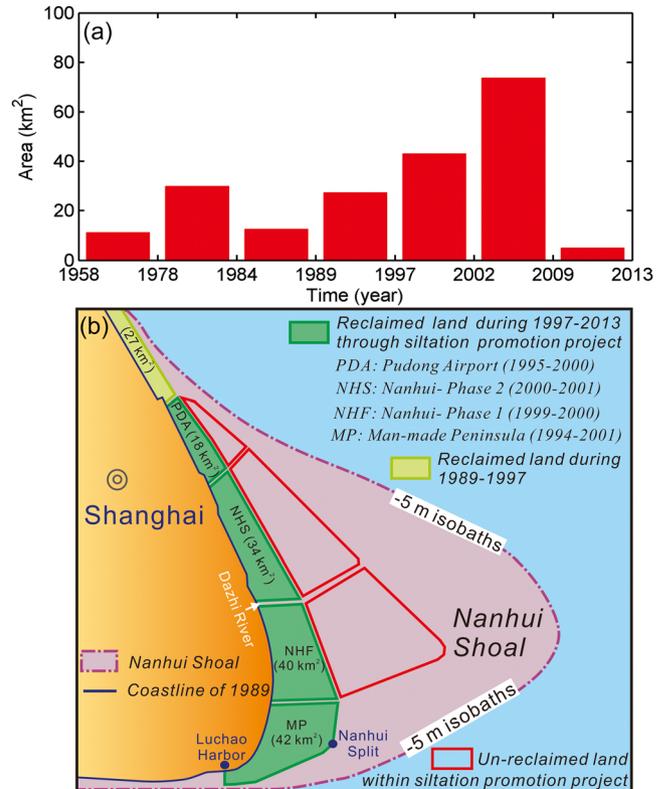


**FIGURE 13** (a) Reclaimed land within the Nanhui Shoal (NHS) over the period 1958–2013 and (b) siltation promotion projects after 1989 [Colour figure can be viewed at wileyonlinelibrary.com]

promotion projects, primarily in the form of underwater groynes, were usually implemented prior to reclamation in the Changjiang Estuary (Li et al., 2007; Liu, Lu, & Cui, 2011); examples include the Pudong Airport Siltation Promotion Project and the Nanhui Siltation Promotion Project (Figure 13b). The siltation promotion projects

became significant after 1994, amounting to an area of 134 km² between 1994 and 2001.

## 4 | DISCUSSION

### 4.1 | Factors impacting the morpho-sedimentary dynamics of estuarine shoals

Considering that increases in both the calculated volume and gross area exceed the calculation errors, the NHS has definitely experienced overall siltation and progradation over the past 55 years, despite the decreased riverine sediment input. Moreover, the only erosion phase, which occurred between 1984 and 1989, is likely attributable to the separation of the Jiangya Shoal (Figures 6 and S4). This differs considerably from widely observed damming-induced delta recession and shoal erosion processes, such these occurring in the Nile (Fanos, 1995) and Mekong deltas (Anthony et al., 2015). The seemingly abnormal phenomenon found in the NHS reveals the uncertainty regarding whether damming leads to sediment starvation in estuaries, the key of which is the sediment source for estuarine deposits. In the Brisbane Estuary in Australia, which receives abundant marine sediments (Eyre, Hossain, & McKee, 1998), and the Changjiang Estuary in this study, which gets supplies of reworked sediments from estuary and outer coast (Dai et al., 2014) and features a stable SSC (Figure 11b) regardless of damming, the link between riverine sediment discharge and shoal evolution is natively weak. In contrast, for estuaries with a strong reliance on terrigenous sediments, such as the Mississippi (Blum & Roberts, 2009) and Po (Simeoni & Corbau, 2009) estuaries, shoal erosion generally occurs in response to damming.

In view of the co-occurrence of intensive siltation promotion actions and the abrupt increase in shoal volume (Figures 8 and 13), the siltation promotion projects likely played a dominant role in recent siltation in the NHS under a regime of decreased riverine sediment input, stable tidal flow regime, and nearly unchanged sedimentary feature (Figures 4 and 6). The engineering-promoted siltation on shoals, mostly through weakening hydrodynamics by construction of infrastructure, has been found to be highly effective, as shown in the Zuiderzee, Netherlands (Hoeksema et al., 2007), the Isahaya Bay, Japan (Hodoki & Murakami, 2006), and the Changjiang Estuary, China (Wei et al., 2015). Thus, the potential link between riverine sediment discharge and shoal evolution is further masked. In addition to the large number of studies on reclamation-induced shoal degradation (e.g., Son & Wang, 2009), the case of the NHS demonstrates a complete evolutionary history of an estuarine shoal under the effects of reclamation projects, with an initial stage characterized by rapid shoal accretion concentrated in the siltation-promotion region and a later stage characterized by a residual narrow shoal after reclamation, and reveals a time lag (of years) between the operation of siltation promotion projects and land reclamation (Figures 13, 14).

Beginning in 1954, the alteration of the Changjiang estuarine regime in response to flood-induced avulsion seems to have controlled changes in the planar geometry of the NHS. In this process, the ebb flow intensity of the South Passage, largely represented by the ebb flow diversion ratio (Dai, Liu, & Wei, 2015) under a stable
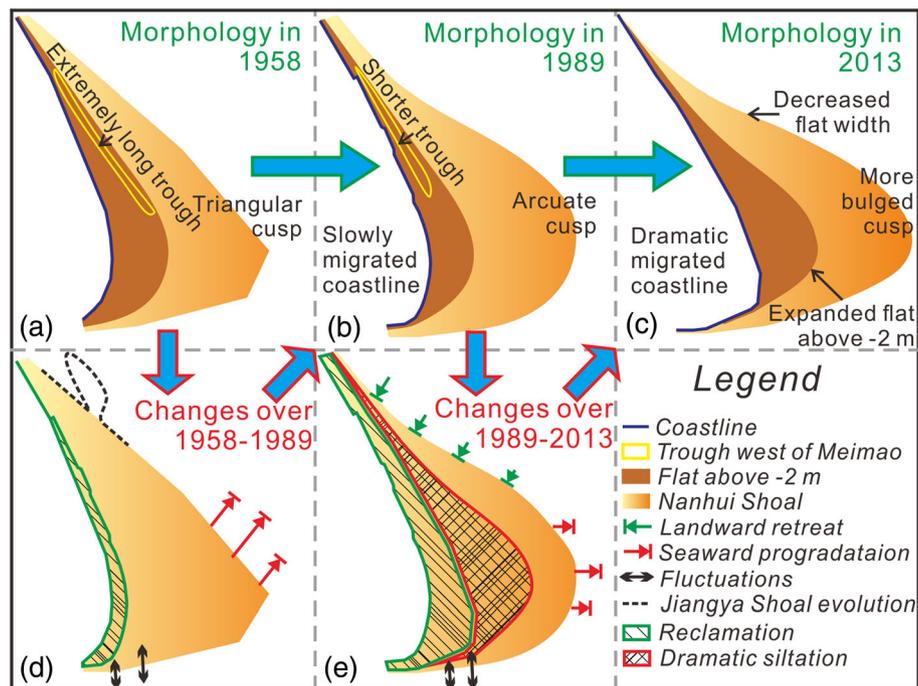


**FIGURE 14** Diagram showing the transition in the multi-decadal evolution of the Nanhui Shoal over the period 1958–2013; (a–c) depict the morphology in 1958, 1989, and 2013 and (d–e) depict the changes from 1958 to 1989 and from 1989 to 2013 [Colour figure can be viewed at wileyonlinelibrary.com]

riverine water discharge (Figure 11a), estuarine tidal range (Dai et al., 2014), and regional tidal flow regime (Figure 4), has exhibited dramatic changes. The shoal geometry has changed accordingly (Figures 6, 7, and 12): a decrease in the ebb flow intensity was generally accompanied by overall shoal progradation (e.g., over 1958–1978), whereas its increase generally triggered southward migration (e.g., over 1984–1989) or seaward progradation (e.g., over 1989–1997; induced by channel straightening) of the shoal cusp. The retreat in the north and progradation around the cusp between 1999 and 2013 resulted from the DWP-induced increase in ebb flow intensity and were supported by the suspended sediment transport mode (Figure 4). The response of the NHS to the estuarine regime adjustment stems from channel–shoal interactions (Scully & Friedrichs, 2007) and indicates the long-lasting impact of extreme events, despite their short duration, in determining the morpho-sedimentary dynamics of estuaries (Mei et al., 2018; Törnqvist, Bick, Klaas, & de Jong, 2006).

## 4.2 | Transition in the multi-decadal evolution of estuarine shoals

The transition in morpho-sedimentary dynamics of estuarine deposits is not unique, especially in the face of climate change and human modifications (Giosan et al., 2014; Syvitski et al., 2009). Perhaps the most typical examples are the widely reported shifts from delta progradation to recession induced by damming (e.g., Anthony et al., 2015; Syvitski et al., 2009) and shifts between wetland degradation and restoration in response to artificial interference (e.g., Kirwan & Megonigal, 2013). Moreover, Syvitski and Saito (2007) identified deserted shoals outside inactive channels in the Huanghe Estuary. Hughes et al. (2009) documented a rapid headward erosion of marsh creeks away from equilibrium in South Carolina under fast sea-level rise. Mei et al. (2018) diagnosed development/disruption cycle in midchannel shoals in relation to extreme floods. For the NHS, a mode of planar geometry alteration regulated by estuarine regime adjustment has been replaced by a mode of landward siltation controlled by estuarine engineering since 1989 (Figure 14). Overall, transition may occur when the factor dominating shoal evolution experiences dramatic changes, such as decreasing riverine sediment input and rising sea level, as in the abovementioned (e.g., Blum & Roberts, 2009), or the dominant factor completely changes, as in this study (Figure 14).

In the most recent decades, intensified artificial interference resulting in marked changes in the normal behavior of estuarine shoals (e.g., van der Wal, Pye, & Neal, 2002) is likely the most important driving factor of the transition. This is ascribed to the intense effects of artificial forcing. For example, damming-induced changes in riverine sediment discharge in recent decades are almost equivalent to those over thousands of years before the 1900s (Syvitski & Milliman, 2007; Wilkinson & McElroy, 2007). Moreover, the morphodynamic behavior triggered by human activities is generally linear and sometimes unnatural, as shown by the continuous delta

recession induced by human activities (e.g., Anthony et al., 2015) and the siltation occurring on the NHS despite the decreased riverine sediment input. This pattern is different from the nonlinear process (alternating deposition and erosion) induced by natural variations, showing real-time mutual feedback between hydrodynamics and shoal morphology (Dam et al., 2016). With multiple artificial interferences becoming increasingly widespread, this study focuses attention on the resultant abnormal morphology, such as the formation of a steeply sloping profile under the combined effects of coastal expansion by reclamation and shoal retreat induced by the DWP, and is not limited to only distinguishing impacts from particular engineering work (e.g., Cuvilliez et al., 2009).

Once a transition occurs, an estuarine shoal will generally break away from the original quasi-equilibrium and evolve towards a new equilibrium state (e.g., Blum & Roberts, 2009; Dam et al., 2016). The transition in the multi-decadal evolution of estuarine shoals can be either harmful (e.g., delta recession and wetland degradation) or beneficial (e.g., wetland restoration), and it is difficult to estimate how long it will take for the shoals to reach a new equilibrium. Further work on the discrimination criteria of transitions, transformation mechanisms, and posttransition morpho-sedimentary dynamics for estuarine shoals should be performed. On this basis, appropriate artificial interference can be conducted to realize a sustainable and effective utilization of resources in estuaries.

## 4.3 | Crisis assessment of estuarine shoals as a resource

Over the period 1958–2013, 202 km$^2$ of land was reclaimed on the NHS (Figure 13), supporting the construction of the Pudong International Airport and development of the Lingang New Town (Li et al., 2007). Meanwhile, the actual tidal flat resource (net area) dramatically decreased (169 km$^2$), although the NHS exhibits a progradation trend with the gross area increasing by 33 km$^2$ (Figures 10 and 13). This pattern reveals a degradation of estuarine shoals under utilitarian reclamation, with the rate of reclamation substantially exceeding the progradation speed of the shoal. Examples can be found in the Saemangeum Reclamation Project, South Korea (Son & Wang, 2009),
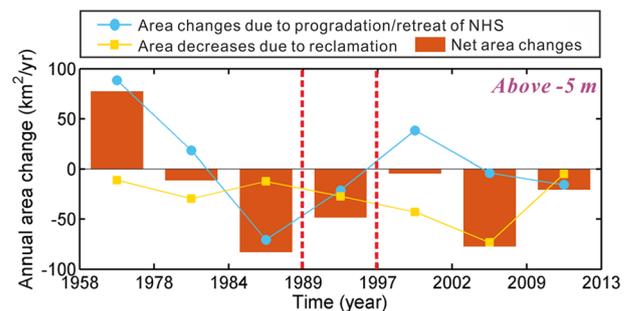
**FIGURE 15** Changes in net area of the NHS in response to progradation/retreat and reclamation. NHS, Nanhui Shoal [Colour figure can be viewed at wileyonlinelibrary.com]
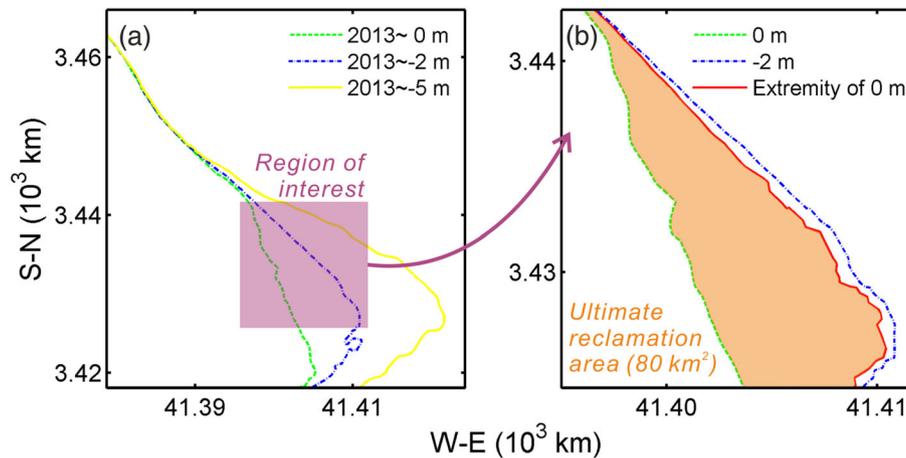
**FIGURE 16** (a) Isobaths of 0, −2, and −5 m of the Nanhui Shoal in 2013, with the region of interest, where steep slopes could be detected in the shoal profile, depicted in purple, and (b) maximum extent of the 0-m isobath progradation under future siltation promotion projects [Colour figure can be viewed at wileyonlinelibrary.com]

and the Isahaya Reclamation Project, Japan (Hodoki & Murakami, 2006), which resulted in decreases in the actual tidal flat area of 401 and 16 km², respectively. Considering the possibly dim future of estuarine shoals in the face of rising sea level, intensified storms, and excessive human activities (Kirwan & Megonigal, 2013), we call for conservative reclamation.

Implications for resource management, important but rarely noticed, can be gained from the multi-decadal morpho-sedimentary dynamics of estuarine shoals. The key factor regulating resource abundance on shoals can vary over the course of their evolution. For example, the tidal flat resource on the NHS is more related to shoal progradation/retreat governed by estuarine regime adjustment during 1958–1989 but depends more on coastline migration controlled by reclamation during 1989–2013 (Figures 14, 15). Moreover, the fining surface sediments on the shoal (Figure 5) and the coarsening sediments outside the estuary (Luo, Yang, & Zhang, 2012) indicate a contribution of eroded fine sediments from the outer coast to the growth of the NHS. Although not the case at present, the shoal is expected to suffer sediment starvation when the supply of erodible sediments from the outer coast becomes insufficient. Furthermore, the formed steep slope entails difficulties for future resource exploitation. Siltation is confined to the region landward of the steep slope by the intense flow of the South Passage, which limits the seaward progradation of the steep slope in the meantime. The siltation will stop when the shore slope reaches a threshold, which depends on the tidal range, the wave height, and the critical velocity for profile stability (Friedrichs, 2011). Here, we attempt to quantify the ultimate land reclamation in the northern section of the NHS above 0 m (Figure 16). Assuming that the location of the steep slope is fixed, the maximum extent of the 0-m isobath progradation is reached when the gradient between 0- and −2-m isobaths meets the threshold, which is spatially different (ranging from 2‰ to 11‰; Figure 9) and set as the gradient of the formed steep slope for each location. This analysis suggests that approximately 80 km² of new land can be reclaimed in the future

(Figure 16). From the above, systematic examinations of the multi-decadal morpho-sedimentary dynamics of estuarine shoals are extremely meaningful for their management.

## 5 | CONCLUSIONS

Estuarine shoals, which have great ecological significance and resource value, have been dramatically affected by the interplay of natural and artificial forcings. In this study, the multi-decadal morpho-sedimentary dynamics of the NHS, the largest marginal shoal of the Changjiang Estuary, are analyzed to determine the response of estuarine shoals to estuarine regime adjustment and multiple artificial interferences and its implications for resource management. The following conclusions are reached:

1. Over the period 1958–2013, the NHS experienced siltation in the landward region, with the volume of the shoal increasing by $4.1 \times 10^8$ m³, and seaward progradation, with the gross areas above 0, −2, and −5 m increasing by 69 km² (33%), 83 km² (26%), and 33 km² (6%), respectively. In relative terms, the tidal flow regime and sedimentary mode around the NHS have changed slightly over the past three decades.

2. A transition occurred in the multi-decadal evolution of the NHS. Dramatic changes took place in the planar geometry of the NHS from 1958 to 1989, with the triangular cusp evolving to an arcuate shape and a bulge forming and then disappearing in the northern section. The landward region experienced significant siltation from 1989 to 2013, whereas the northern section of the NHS gradually retreated. Accordingly, an extremely steep slope with grades of 2–11‰ formed in the shoal profile by 2013.

3. The alterations in the ebb flow intensity of the South Passage induced by the estuarine regime adjustment controlled the morpho-sedimentary dynamics of the NHS from 1958 to 1989. The large-scale siltation promotion projects induced significant

landward sedimentation on the NHS from 1989 to 2013. The decrease in the riverine sediment input driven by the TGD has played a limited role in the accretion of the shoal.

4. Despite the overall trend of seaward progradation, the reclamation of 202 km$^2$ has resulted in a 29% reduction in the tidal flat resource of the NHS over the period 1958–2013. The steeply sloping profile formed within the NHS entails difficulties for future resource exploitation; only a maximum of 80 km$^2$ of land can be reclaimed in the future.

5. The multi-decadal morpho-sedimentary dynamics of the NHS show that human activities have replaced natural variations as the dominant factor in recent estuarine shoal evolution. Thus, systematic examinations of the morpho-sedimentary dynamics of shoals under the influence of both natural and artificial forcings, preferably over relatively long (multi-decadal) time scales, are necessary for evaluating future changes and their implications for shoal management and exploitation (notably siltation promotion and reclamation projects).

## ORCID

*Zhijun Dai* https://orcid.org/0000-0001-7682-0310

## REFERENCES

Abam, T. K. S. (1999). Impact of dams on the hydrology of the Niger Delta. *Bulletin of Engineering Geology and the Environment*, 57(3), 239–251. https://doi.org/10.1007/s100640050041

Anthony, E. J., Almar, R., & Aagaard, T. (2016). Recent shoreline changes in the Volta River delta, West Africa: The roles of natural processes and human impacts. *African Journal of Aquatic Science*, 41(1), 81–87. https://doi.org/10.2989/16085914.2015.1115751

Anthony, E. J., Brunier, G., Besset, M., Goichot, M., Dussouillez, P., & Nguyen, V. L. (2015). Linking rapid erosion of the Mekong River delta to human activities. *Scientific Reports*, 5, 14745. https://doi.org/10.1038/srep14745

Bergillos, R. J., Rodríguez-Delgado, C., Millares, A., Ortega-Sánchez, M., & Losada, M. A. (2016). Impact of river regulation on a Mediterranean delta: Assessment of managed versus unmanaged scenarios. *Water Resources Research*, 52(7), 5132–5148. https://doi.org/10.1002/2015WR018395

Blott, S. J., Pye, K., van der Wal, D., & Neal, A. (2006). Long-term morphological change and its causes in the Mersey Estuary, NW England. *Geomorphology*, 81(1–2), 185–206. https://doi.org/10.1016/j.geomorph.2006.04.008

Blum, M. D., & Roberts, H. H. (2009). Drowning of the Mississippi Delta due to insufficient sediment supply and global sea-level rise. *Nature Geoscience*, 2(7), 488–491. https://doi.org/10.1038/ngeo553

Canestrelli, A., Lanzoni, S., & Fagherazzi, S. (2014). One-dimensional numerical modeling of the long-term morphodynamic evolution of a tidally-dominated estuary: The Lower Fly River (Papua New Guinea). *Sedimentary Geology*, 301(3), 107–119. https://doi.org/10.1016/j.sedgeo.2013.06.009

Chen, J. T., & Yang, F. D. (2010). Observation experiment and analysis between fathometer and sounding pole. *Yellow River*, 32(10), 57–59. (In Chinese)

Cuvilliez, A., Deloffre, J., Lafite, R., & Bessineton, C. (2009). Morphological responses of an estuarine intertidal mudflat to constructions since 1978 to 2005: The Seine estuary (France). *Geomorphology*, 104(3–4), 165–174. https://doi.org/10.1016/j.geomorph.2008.08.010

Dai, Z., Fagherazzi, S., Mei, X., Chen, J., & Meng, Y. (2016). Linking the infilling of the North Branch in the Changjiang (Yangtze) estuary to anthropogenic activities from 1958 to 2013. *Marine Geology*, 379, 1–12. https://doi.org/10.1016/j.margeo.2016.05.006

Dai, Z., Liu, J. T., Wei, W., & Chen, J. (2014). Detection of the Three Gorges Dam influence on the Changjiang (Yangtze River) submerged delta. *Scientific Reports*, 4, 6600.

Dai, Z. J., Liu, J. T., & Wei, W. (2015). Morphological evolution of the South Passage in the Changjiang (Yangtze River) estuary, China. *Quaternary International*, S, 380–381, 314–326.

Dam, G., van der Wegen, M., Labeur, R. J., & Roelvink, D. (2016). Modeling centuries of estuarine morphodynamics in the Western Scheldt estuary. *Geophysical Research Letters*, 43(8), 3839–3847. https://doi.org/10.1002/2015GL066725

Daniel, R. L. (1985). Analysis test cases for three dimensional hydrodynamic models. *International Journal for Numerical Methods in Fluids*, 5, 529–543.

Eyre, B., Hossain, S., & McKee, L. (1998). A suspended sediment budget for the modified subtropical Brisbane River Estuary, Australia. *Estuarine, Coastal and Shelf Science*, 47, 513–522. https://doi.org/10.1006/ecss.1998.0371

Fanos, A. M. (1995). The impact of human activities on the erosion and accretion of the Nile Delta coast. *Journal of Coastal Research*, 11(3), 821–833.

Folk, R. L., & Ward, W. C. (1957). Brazos river bar, a study in the significance of grain size parameter. *Journal of Sedimentary Research*, 27(1), 3–26. https://doi.org/10.1306/74D70646-2B21-11D7-8648000102C1865D

Friedrichs, C. T. (2011). Tidal flat morphodynamics: A synthesis. In J. D. Hansom, & B. W. Flemming (Eds.), *Treatise on estuarine and coastal science, volume 3: Estuarine and coastal geology and geomorphology* (p. 34). Elsevier. https://doi.org/10.1016/B978-0-12-374711-2.00307-7

Giosan, L., Syvitski, L., Constantinescu, S., & Day, J. (2014). Climate change: Protect the world's deltas. *Nature*, 516(7529), 31–33. https://doi.org/10.1038/516031a

Hodoki, Y., & Murakami, T. (2006). Effects of tidal flat reclamation on sediment quality and hypoxia in Isahaya Bay. *Aquatic Conservation Marine & Freshwater Ecosystems*, 16(6), 555–567. https://doi.org/10.1002/aqc.723

Hoeksema, R. J., Vlotman, W. F., & Madramootoo, C. A. (2007). Three stages in the history of land reclamation in the Netherlands. *Irrigation & Drainage*, 56, S113–S126. https://doi.org/10.1002/ird.340

Hu, K. L., & Ding, P. X. (2009). The effect of deep waterway constructions on hydrodynamics and salinities in Yangtze Estuary, China. *Journal of Coastal Research*, 56, 961–965.

Hughes, Z. J., Fitzgerald, D. M., Wilson, C. A., Pennings, S. C., Wieski, K., & Mahadevan, A. (2009). Rapid headward erosion of marsh creeks in response to relative sea level rise. *Geophysical Research Letters*, 36, 441–451.

Kim, T. I., Choi, B. H., & Lee, S. W. (2006). Hydrodynamics and sedimentation induced by large-scale coastal developments in the Keum River Estuary, Korea. *Estuarine Coastal & Shelf Science*, 68(3–4), 515–528. https://doi.org/10.1016/j.ecss.2006.03.003

Kirwan, M. L., & Megonigal, J. P. (2013). Tidal wetland stability in the face of human impacts and sea-level rise. *Nature*, 504, 53–60. https://doi.org/10.1038/nature12856

Li, J. F., Dai, Z. J., Ying, M., Wu, R. R., Fu, G., & Xu, H. G. (2007). Analysis on the development and evolution of tidal flats and reclamation of land resource along shore of Shanghai city. *Journal of Natural Resources*, 22(3), 361–371. (In Chinese)

Liu, X. C., Lu, Y. J., & Cui, D. (2011). Analysis on development and layout of land-water resources of Eastern Nanhui Beach and its impacts on river regime. *Water Resources Planning and Design*, 6, 9–13. (In Chinese)

Luo, X. X., Yang, S. L., & Zhang, J. (2012). The impact of the Three Gorges Dam on the downstream distribution and texture of sediments along the middle and lower Yangtze River (Changjiang) and its estuary, and subsequent sediment dispersal in the East China Sea. *Geomorphology*, 179(1), 126–140. https://doi.org/10.1016/j.geomorph.2012.05.034

Mei, X. F., Dai, Z. J., Wei, W., Li, W. H., Wang, J., & Sheng, H. (2018). Secular bathymetric variations of the North Channel in the Changjiang (Yangtze) Estuary, China, 1880–2013: Causes and effects. *Geomorphology*, 303, 30–40. https://doi.org/10.1016/j.geomorph.2017.11.014

Pittaluga, B. M., Tambroni, N., Canestrelli, A., Slingerland, R., Lanzoni, S., & Seminara, G. (2015). Where river and tide meet: The morphodynamic equilibrium of alluvial estuaries. *Journal of Geophysical Research Earth Surface*, 120(1), 75–94. https://doi.org/10.1002/2014JF003233

Pranzini, E. (2001). Updrift river mouth migration on cuspate deltas: Two examples from the coast of Tuscany (Italy). *Geomorphology*, 38(1–2), 125–132. https://doi.org/10.1016/S0169-555X(00)00076-3

Qiao, H. J., Zhang, J. Y., & Xu, X. M. (2010). Discussion on calculation method of tidal shear velocity and roughness length in Yangtze River estuary. *Journal of China Hydrology*, 30(4), 23–28. (In Chinese)

Rossington, S. K., Nicholls, R. J., Stive, M. J. F., & Wang, Z. B. (2011). Estuary schematisation in behaviour-oriented modelling. *Marine Geology*, 281(1), 27–34. https://doi.org/10.1016/j.margeo.2011.01.005

Sabatier, F., Maillet, G., Provansal, M., Fleury, T. J., Suanez, S., & Vella, C. (2006). Sediment budget of the Rhône delta shoreface since the middle of the 19th century. *Marine Geology*, 234(1–4), 143–157. https://doi.org/10.1016/j.margeo.2006.09.022

Scully, M. E., & Friedrichs, C. T. (2007). The importance of tidal and lateral asymmetries in stratification to residual circulation in partially mixed estuaries. *Journal of Physical Oceanography*, 37(6), 1496–1511. https://doi.org/10.1175/JPO3071.1

Simeoni, U., & Corbau, C. (2009). A review of the Delta Po evolution (Italy) related to climatic changes and human impacts. *Geomorphology*, 107(1–2), 64–71. https://doi.org/10.1016/j.geomorph.2008.11.004

Son, S. H., & Wang, M. (2009). Environmental responses to a land reclamation project in South Korea. *Eos Transactions American Geophysical Union*, 90(44), 398–399. https://doi.org/10.1029/2009EO440002

Stouthamer, E., & Berendsen, H. J. A. (2001). Avulsion frequency, avulsion duration, and interavulsion period of Holocene channel belts in the Rhine-Meuse delta, the Netherlands. *Nederlandse Geografische Studies*, 71(283), 105–126.

Syvitski, J. P. M., Kettner, A. J., Overeem, I., Hutton, E. W. H., Hannon, M. T., Brakenridge, G. R., ... R. J. (2009). Sinking deltas due to human activities. *Nature Geoscience*, 2(10), 681–686. https://doi.org/10.1038/ngeo629

Syvitski, J. P. M., & Milliman, J. D. (2007). Geology, geography, and humans battle for dominance over the delivery of fluvial sediment to the coastal ocean. *The Journal of Geology*, 115, 1–19. https://doi.org/10.1086/509246

Syvitski, J. P. M., & Saito, Y. (2007). Morphodynamics of deltas under the influence of humans. *Global & Planetary Change*, 57(3–4), 261–282. https://doi.org/10.1016/j.gloplacha.2006.12.001

Tatui, F., Vespremeanu-Stroe, A., & Preoteasa, L. (2014). Alongshore variations in beach-dune system response to major storm events on the Danube Delta coast. *Journal of Coastal Research*, 70(sp1), 693–699. https://doi.org/10.2112/SI70-117.1

Todeschini, I., Toffolon, M., & Tubino, M. (2008). Long-term morphological evolution of funnel-shape tide-dominated estuaries. *Journal of Geophysical Research Oceans*, 113, C05005.

Törnqvist, T. E., Bick, S. J., Klaas, V. D. B., & de Jong, A. F. M. (2006). How stable is the Mississippi Delta? *Geology*, 34(8), 697–700. https://doi.org/10.1130/G22624.1

Törnqvist, T. E., Kidder, T. R., Autin, W. J., van der Borg, K., van Dam, R. L., & Wiemann, M. C. (1996). A revised chronology for Mississippi River subdeltas. *Science*, 273(5282), 1693–1696. https://doi.org/10.1126/science.273.5282.1693

van der Wal, D., & Pye, K. (2003). The use of historical bathymetric charts in a GIS to assess morphological change in estuaries. *Geographical Journal*, 169(1), 21–31.

van der Wal, D., Pye, K., & Neal, A. (2002). Long-term morphological change in the Ribble Estuary, northwest England. *Marine Geology*, 189(3–4), 249–266.

Verney, R., Lafite, R., & Bruncottan, J. C. (2009). Flocculation potential of estuarine particles: The importance of environmental factors and of the spatial and seasonal variability of suspended particulate matter. *Estuaries & Coasts*, 32(4), 678–693. https://doi.org/10.1007/s12237-009-9160-1

Wei, W., Dai, Z. J., Mei, X. F., Liu, J. P., Gao, S., & Li, S. S. (2017). Shoal morphodynamics of the Changjiang (Yangtze) estuary: Influences from river damming, estuarine hydraulic engineering and reclamation projects. *Marine Geology*, 386, 32–43. https://doi.org/10.1016/j.margeo.2017.02.013

Wei, W., Mei, X. F., Dai, Z. J., & Tang, Z. H. (2016). Recent morphodynamic evolution of the largest uninhibited island in the Yangtze (Changjiang) estuary during 1998–2014: Influence of the anthropogenic interference. *Continental Shelf Research*, 124, 83–94. https://doi.org/10.1016/j.csr.2016.05.011

Wei, W., Tang, Z. H., Dai, Z. J., Lin, Y. F., Ge, Z. P., & Gao, J. J. (2015). Variations in tidal flats of the Changjiang (Yangtze) estuary during 1950s–2010s: Future crisis and policy implication. *Ocean & Coastal Management*, 108, 89–96. https://doi.org/10.1016/j.ocecoaman.2014.05.018

Wilkinson, B., & McElroy, B. (2007). The impact of humans on continental erosion and sedimentation. *Geological Society of America Bulletin*, 119, 140–156. https://doi.org/10.1130/B25899.1

Wright, L. D., & Coleman, J. M. (1974). Mississippi River mouth processes: Effluent dynamics and morphologic development. *Journal of Geology*, 82(6), 751–778. https://doi.org/10.1086/628028

Yang, S. L., Milliman, J. D., Li, P., & Xu, K. (2011). 50,000 dams later: Erosion of the Yangtze River and its delta. *Global & Planetary Change*, *75*(1), 14–20. https://doi.org/10.1016/j.gloplacha.2010.09.006

Yun, C. X. (2010). *Illustrated handbook on evolution of Yangtze estuary*. Beijing: China Ocean Press. (In Chinese)

Zhang, M., Townend, I., Zhou, Y. X., & Cai, H. Y. (2016). Seasonal variation of river and tide energy in the Yangtze estuary, China. *Earth Surface Processes & Landforms*, *41*(1), 98–116. https://doi.org/10.1002/esp.3790

Zhang, W. H. (1988). Calculation of unit-width suspended sediment transportation rate. *Journal of China Hydrology*, *2*, 22–27. (In Chinese)

## SUPPORTING INFORMATION

Additional supporting information may be found online in the Supporting Information section at the end of the article.